

PROGRESSIVE TRANSMISSION AND RENDERING OF FOVEATED VOLUME DATA

Chen Chen, Zhiyong Huang, Hang Yu, Ee-Chien Chang
Department of Computer Science, School of Computing
National University of Singapore, Singapore 117543
Email: {chenche1,huangzy,yuhang,change1}@comp.nus.edu.sg

Keywords: Progressive Transmission and Volume Rendering, Wavelet Foveation, Multiresolution.

Abstract: With development of biomedical and networking technology, interactive volume rendering with data transmitted via the network becomes an interesting topic. Two technical problems are data transmission and fast volume rendering. In this paper, two schemes using Wavelet foveation are proposed and implemented: the region-based and coarse-to-fine. The first scheme transmits and renders the region of interest (ROI) of volume data on the client site at highest resolution for the first time, and consequently it iteratively expands the region layer by layer towards to the peripheral. While the second one gives a complete image in a low resolution for the first time on the client. The detail coefficients will be transmitted continuously and the rendering result will be progressively refined depending on the distance to the ROI.

1 Introduction

Modern scanners such as CT and MRI provide detailed cross-sections of objects at a very high resolution. These data sets occupy huge amount of memory space. Some super computer centers maintain large data repositories on servers whose data sets will be accessed through networks and rendered on clients for researchers around the world to collaborate in their research (Hancock and Hubbard, 1997) (Bhaniramka and Demange, 2002).

The network's bandwidth is relatively low for the large scientific data sets. Lossy compression is typically employed to reduce data size. However, for very large data sets, such reduction is still insufficient, especially when interactivity is required. Region of interest (ROI) is another approach to further reduce the data size. The ROI is determined from the user's intention, which in turns prioritizes the data transmission. Hence, a few design issues are on how to translate the user's interactive feedback to the transmission order of the data, and how to render and present the partial information received in the client's side. The above design issues are the focus of this paper.

Many state-of-the-art lossy image compression schemes are based on Wavelet transform. For natural images and many medical volume data sets, a large number of their Wavelet coefficients have small val-

ues. The lossy compression is obtained by discarding coefficients lower than a threshold, and such threshold determines the quality and compression rate. To compress with ROI, different thresholds are set for coefficients correspond to different spatial location. A foveated volume can be viewed as a volume with multiple levels of ROI. The spatial resolution is highest at a location known as fovea, but decrease gradually for as the distance from the fovea increases.

We adopt the following approach of interactive transmission and rendering. The Wavelet coefficients are progressively transmitted by the server and progressively rendered by the client, in an order determined by the location of the fovea indicated by the user. There are two ways of progressive transmission/rendering. One is region-based, that is, the priority of an coefficient will be inversely proportional to its distance to the center fovea. The center fovea will have the highest priority thus will be transmitted and rendered first on client site with highest resolution. The user on the client site will see a small portion of the volume which he/she is most interested in. It will then be expanded progressively until the whole foveated volume is received (Figures 11 and 13). The other one is coarse-to-fine scheme. The volume in lowest resolution will be transmitted and rendered first. More coefficients will arrive successively to refine region near the fovea Thus, the user will first

Methods	RB	O	DA	CR	RSV	PR
1	n	1	1	-	-	n
2	y	2	2	m	O(n)	n
3	y	2	2	m	O(1)	n
4	y	2	2	h	O(1)	n
5	y	3	3	h	O(log n)	n
6	y	4	3	m	O(log n)	y

Table 1: Comparison of various data preprocessing methods: 1(Lacroute and Levoy, 1994), 2(Gross et al., 1997), 3(Ihm and Park, 1998), 4(Kim and Shin, 1999), 5(Guthe et al., 2002), 6(Norton and Rockwood, 2003) (Wavelet-Based (WB): y=yes, n=no. Output (O): 1-a list of voxel scan-line, 2-the whole data set, 3-the significant and near cubes, 4-the coefficients of the visible frontal cubes; Data Access (DA): 1-sequential, 2-random, 3-hierarchical; Compression Rate (CR): -not applicable, l-low, m-medium, h-high; Reconstruction of a Single Voxel (RSV); Progressive Refinement (PR): y=yes, n=no)

see a low resolution image, and next an image with 2 levels of details, follow by 3 levels of details and so forth (Figures 12 and 14). We have implemented the above two transmission/rendering schemes. The results are compared and reported.

2 Related work

The huge amount of data is the most significant problem both in data transmission and volume rendering. The technical solution includes data compression and fast volume rendering.

Many researchers employed Wavelet transform in their compression schemes for volume rendering. They usually contain four steps: Wavelet transform, normalization, thresholding, and encoding. First, transform the data into Wavelet domain. Second, the Wavelet coefficients are normalized to the interval [0,1]. Third, those coefficients that are smaller than a certain threshold value are discarded. Fourth, the data are encoded using some coding schemes like run-length or Huffman. Data extraction is employed further to extract the most important data and transfer with priority for rendering. A comparison of some compression methods is listed in Table 1.

There are four techniques that are particular popular in volume rendering: raycasting, splatting, shear-warp and texture-mapping hardware-based approaches (Meissner et al., 2000). Raycasting and splatting give better image quality but have lower rendering speed. Raycasting casts a ray for each image pixel into the volume and accumulate the sample value along the ray by resampling. In contrast with ray casting, splatting, first proposed in (West-

Methods	OR	OQ	RA	RS	MC
1	u	l	1	$3 * n(slice)$ $*n(voxel_in_slice)$	m
2	u	m	2	$n(slice)$ $*n(voxel_in_slice)$	h
3	m	m	2	$n(slice)$ $*n(voxel_in_slice)$	l
4	u	h	3	$n(voxel)-$ $n(transparent)$	h
5	u	h	3	$n(voxel)$ $-n(transparent)$	m

Table 2: Comparison of various rendering methods: 1(Pinnamaneni et al., 2002), 2(Pinnamaneni, 2003), 3(Guthe et al., 2002), 4(Lacroute and Levoy, 1994), 5(Kim and Shin, 1999) (Output Resolution (OR): u-uniform, m-multiresolution; Output Quality (OQ): l-low, m-medium, h-high; Rendering Algorithm (RA): 1-2D texture mapping, 2-3D texture mapping, 3-shear-warp; Rendering Time Complexity (RTC); Rendering Space Complexity (RSC): l-low, m-medium, h-high)

over, 1990), is a feed forward algorithm calculating the footprint which is the weight of the voxel contributing to its neighboring pixel. Both methods have been combined with Wavelet transform in order to reduce the size of volume data to fit into core memory (Westenberg and Roerdink, 2000) (Gross et al., 1997).

Texture-mapping is a hardware based method which is very fast but gives lower image quality. When the data set is too large that the texture is hard to be loaded totally into texture memory, texture swap will occur and rendering speed will reduce dramatically. Shear-warp (Lacroute and Levoy, 1994) is the fastest software-based algorithm and gives similar image quality with raycasting and splatting. However, when the magnification is high, significant aliasing is present. A comparison of some methods is listed in Table 2. The image quality has been significantly improved in (Engel et al., 2001).

3 Our work

Our method contains three steps: data preprocessing, progressive transmission and progressive volume rendering.

Volume data is first transformed to Wavelet form and divided into 8x8x8 blocks, each block is encoded using RLE (run-length encoding) in server site. Blockwise structure is employed in order to enable efficient data compression as well as convenient communication between server and client. When a client request is received, a compressed foveated volume is extracted. A foveated volume has highest resolution

at the fovea while the resolution falls off when the distance with the fovea increases. We use Wavelet foveation to approximate foveation operator (Chang et al., 2000). For an original data set with size 1024^3 and fovea size 48^3 , the Wavelet foveated volume will have approximately $24^3 * 36 = 497664$ coefficients, which is reduced by a factor of 2,000 comparing with the original size. Details of Wavelet transform and extraction of foveated volume will be described in subsections 3.1.1 and 3.1.2.

Data is then progressively transmitted in sequence. Data blocks of the Wavelet foveated volume are reordered according to two priority assignment schemes: region-based and the coarse-to-fine. They will be discussed in detail in subsection 3.2.

To be consistent with progressive data transmission, progressive rendering algorithm is employed. In region-based scheme, the volume are displayed on client site layer by layer from fovea toward the peripheral. The fovea area will be rendered in high resolution using data received earlier and in each successive step, one immediate outer layer is displayed in half resolution of its inner layer. In coarse-to-fine scheme, the client will first show a rough average image of the volume and iteratively refines the fovea area. Two progressive rendering algorithms are described in subsection 3.3.1. Viewing from a non-orthogonal direction will be discussed in subsection 3.3.2.

3.1 Data preprocessing

3.1.1 Data compression

Haar Wavelet is implemented because it is simple and has a good correspondence with octree that enables easy data searching and reconstruction.

Haar Wavelet transform We will illustrate it in 2D case first. Let I be an image of size $2^N \times 2^N$. Four images can be generated from I after one pass of Haar Wavelet transform, where

$$\begin{aligned} I_{00}(i, j) &= \frac{I(2i, 2j) + I_{10}(i, j) + I_{01}(i, j) + I_{11}(i, j)}{4} \\ I_{10}(i, j) &= I(2i + 1, 2j) \\ I_{01}(i, j) &= I(2i, 2j + 1) \\ I_{11}(i, j) &= I(2i + 1, 2j + 1) \\ i, j &= 0 \dots 2^{N-1} - 1 \end{aligned}$$

As illustrated in Figure 1, image I_{00} is an average image of image I with half resolution. The rest three images are called detail images. We recursively perform this process on the average image of each iteration until the average image has only 1 pixel or reaches some pre-defined resolution. The result will be the Wavelet representation of the original image I .

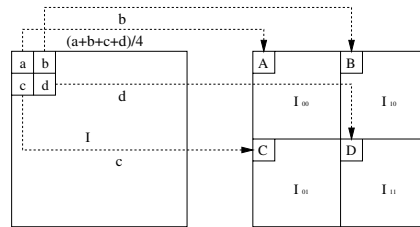


Figure 1: Illustration of Wavelet transform.

L0		L1		L2			
A ₀₀	A ₀₁	HL ₀₀	HL ₀₁	HL ₀₀	HL ₀₁	HL ₀₂	HL ₀₃
A ₁₀	A ₁₁	HL ₁₀	HL ₁₁	HL ₁₀	HL ₁₁	HL ₁₂	HL ₁₃
LH ₀₀	LH ₀₁	HH ₀₀	HH ₀₁	HL ₂₀	HL ₂₁	HL ₂₂	HL ₂₃
LH ₁₀	LH ₁₁	HH ₁₀	HH ₁₁	HL ₃₀	HL ₃₁	HL ₃₂	HL ₃₃
LH ₀₀	LH ₀₁	LH ₀₂	LH ₀₃	HH ₀₀	HH ₀₁	HH ₀₂	HH ₀₃
LH ₁₀	LH ₁₁	LH ₁₂	LH ₁₃	HH ₁₀	HH ₁₁	HH ₁₂	HH ₁₃
LH ₂₀	LH ₂₁	LH ₂₂	LH ₂₃	HH ₂₀	HH ₂₁	HH ₂₂	HH ₂₃
LH ₃₀	LH ₃₁	LH ₃₂	LH ₃₃	HH ₃₀	HH ₃₁	HH ₃₂	HH ₃₃

Figure 2: Wavelet Transform of a $(8k)^2 * blk_sz$ data set

Blockwise hierarchical compression scheme In the server site, we use a blockwise hierarchical compression scheme similar to (Guthe et al., 2002). Divide the volumes into blocks of $(2k)^3$, then apply generic Haar Wavelet transform on it to get 8 blocks of size k^3 . One of them will be average block, the other 7 are detail blocks. Group 8 adjacent average blocks again to obtain a block of size $(2k)^3$. Repeat this procedure until the size of the average image reaches m . These m blocks are the low pass filtered volume of the whole volume data. The value of k has a tradeoff between compression rate and data redundancy during transmission. Since the block will be regarded as a unit during data transmission. Large k value will cause data redundancy since we will transmit more data than we actually needed. Small k value usually gives low compression rate. In our case, k will be 8 and m will be 16.

Give a 2D data set of size $(8k)^2 * blk_sz$, repeat the procedure described previously 2 times and obtain 4 average blocks marked as A_{00}, A_{01}, A_{10} and A_{11} (Figure 2). Each of them associates with a quadtree (Figure 3). Take A_{00} as example, the coefficients marked in grey color are all the component nodes in quadtree of A_{00} . Local coordinate in a level v corresponds with 3 blocks: HL, LH and HH, which are the 3 components of node (v, i, j) in the quadtree. Four child nodes of this node (v, i, j) in level $v+1$ can be simply identified by $(2i, 2j)$, $(2i, 2j+1)$, $(2i+1, 2j)$ and $(2i+1, 2j+1)$, which forms a pointless quadtree.

3D case is almost the same with 2D, the only difference is each node will have 7 component nodes: LLH, LHL, LHH, HLL, HLH, HHL and HHH, and each node has 8 child nodes.

After Wavelet volume are divided into data blocks. RLE(run-length encoding) is performed on it block by block in order of front to back, top to bottom and left to right. The compressed block is a list of value(v) and length(l) pairs.

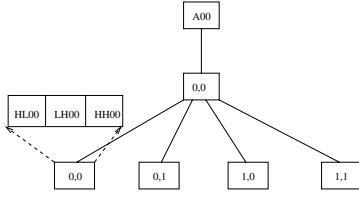


Figure 3: Quadtree of data set in Figure 2.

3.1.2 Derive foveated volume in Wavelet domain

Having a volume W in Wavelet domain and ROI defined by a viewer, we need to derive the foveated volume W_f . The ROI is defined as $ROI\{(x, y, z), r^3\}$, where (x, y, z) is the center of fovea and r indicates its region.

The lowest resolution image of W is defined as layer 0 image, and the second lowest resolution image as layer 1 image and so on. layer 0 is actually the average image of W , and layer i image can be obtained by performing inverse Wavelet transform to layer $i-1$ with the corresponding detailed coefficients (corresponding detailed coefficients are layer i details). The highest resolution image in W is denoted as layer max_layer . In general, the volume data is of size $W*H*D$, and the size of the lowest resolution layer is $\frac{W}{m} * \frac{H}{m} * \frac{D}{m}$ (assuming W, H and D are multiples of m and m is power of 2). In case the volume data V is cubic with size of N^3 (N is power of 2), and the Wavelet transform is processed until the average image has size m^3 , $m_L = \log_2 \frac{N}{m}$.

W_f is extracted from W . It consists of all voxels that are needed for reconstructing ROI_i , where ROI_i is the region of interest in the i th layer of W . The center of ROI_i is $(\lfloor \frac{x}{2^{m_L-i}} \rfloor, \lfloor \frac{y}{2^{m_L-i}} \rfloor, \lfloor \frac{z}{2^{m_L-i}} \rfloor)$ and the size of ROI_i is r^3 .

For convenience of calculation, the boundary of ROI_i can be defined as

$$begin_i.x = (x/2^{(m_L-i)} - s/2) \oplus (0XFFFE) \quad (1)$$

$$begin_i.y = (y/2^{(m_L-i)} - s/2) \oplus (0XFFFE) \quad (2)$$

$$begin_i.z = (z/2^{(m_L-i)} - s/2) \oplus (0XFFFE) \quad (3)$$

$$end_i.x = (x/2^{(m_L-i)} + s/2) \oplus (0XFFFE) - 1 \quad (4)$$

$$end_i.y = (y/2^{(m_L-i)} + s/2) \oplus (0XFFFE) - 1 \quad (5)$$

$$end_i.z = (z/2^{(m_L-i)} + s/2) \oplus (0XFFFE) - 1 \quad (6)$$

$$begin_i.t, end_i.t \in [0, minlen * 2^i - 1], t = x, y, z$$

Figure 4 gives a 2D example of $ROI=\{(9,9),6\}$ for a $16*16$ image, where $m=1$, that is, the average image size is 1^2 . In this example, $m_L = \log_2 16 = 4$. Take layer 3 as an example, $ROI_3 = \{(4,4),6\}$, pixels in layer 3 image with coordinate (i,j) , $i, j \in [2,7]$ are in ROI_3 . In order to reconstruct ROI_3 , layer 3 details with coordinate (i,j) , $i, j \in [1,3]$ are needed. Figure 4(b) represents the reconstructed foveated image.

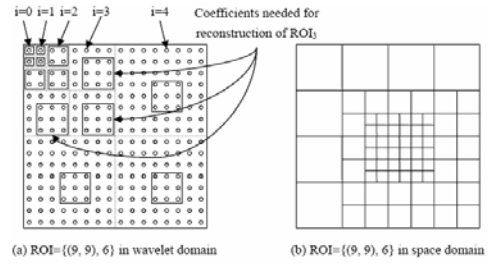


Figure 4: Extraction of the foveated data in Wavelet domain.

3.2 Progressive transmission

Progressive transmission is to re-order the coefficients such that more important coefficients will be regarded as high priority and being sent first. These coefficients can be rendered in the client site separately with other data. Less important coefficients will be sent progressively, step by step, to refine the result image.

There are two ways of progressive transmission in Wavelet volume rendering schemes: the region-based and coarse-to-fine.

The first method is intuitive to implement. We just send the Wavelet foveated volume data from inner layer to outer layer progressively. Coefficients in each layer should be wrapped as an atomic package.

The basic idea of the second method is to send all data blocks for constructing ROI_i in each iteration. At the first iteration, boundary of ROI_{m_L} will be computed and data blocks in layer $m_L - 1$ that contain coefficients for ROI_{m_L} will be added into the data queue. All parent blocks of these blocks will also be added into the data queue. A block is regarded as a parent block of another block if it's a parent node of that block in the octree they belong to. The index of the data block will be added into the data list when it is added into the data queue. In iteration i , boundary of ROI_{m_L-i+1} will be computed. Data blocks in layer $m_L - i$ that contain coefficients for ROI_{m_L-i+1} and all parent blocks of these blocks will be added into the data queue if that block does not exist in the data list. Repeat this procedure until coefficients of ROI_0 are added into the data queue. If the data list doesn't contain all data blocks in average image after above procedure, append the remaining average blocks into the data queue.

Let's illustrate the procedure using a 2D example. Given a 2D image with size $128 * 128$, where $m=16$, $k=8$ and $ROI=(86,86),45$. The average image has size $16 * 16$, which contains 4 data blocks, the fovea centered at coordinate $(86,86)$ with size $(45,45)$. In this example, $m_L = \log_2(128/16) = \log_2 8 = 3$.

Take ROI_2 as an example, $ROI_2 = \{(\lfloor \frac{x}{2^{m_L-i}} \rfloor, \lfloor \frac{y}{2^{m_L-i}} \rfloor), d\} = \{(\lfloor \frac{86}{2^2} \rfloor, \lfloor \frac{86}{2^2} \rfloor), 45\} = \{(43, 43), 45\}$.

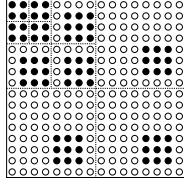


Figure 5: Wavelet foveated image.

$$\begin{aligned}
 begin_i.x &= (43 - 45/2) \oplus (0XFFFE) = 20 \\
 begin_i.y &= (43 - 45/2) \oplus (0XFFFE) = 20 \\
 end_i.x &= (43 + 45/2) \oplus (0XFFFE) - 1 = 63 \\
 end_i.y &= (43 + 45/2) \oplus (0XFFFE) - 1 = 63 \\
 &begin_i.x, begin_i.y, end_i.x, end_i.y \in [0, 63]
 \end{aligned}$$

Pixels in layer 2 image with coordinate (i, j) , $i, j \in [20, 63]$ are in ROI_2 . In order to reconstruct ROI_2 , layer 2 details with local coordinates (i, j) , $i, j \in [10, 31]$ are needed, represented as block index (blk_i, blk_j) , $blk_i, blk_j \in [1, 3]$. Similarly, $ROI_3 = \{(86, 86), 45\} = [64, 107]$, level 3 details: (blk_i, blk_j) , $blk_i, blk_j \in [4, 6]$ $ROI_2 = \{(43, 43), 45\} = [20, 63]$, level 2 details: (blk_i, blk_j) , $blk_i, blk_j \in [1, 3]$ $ROI_1 = \{(21, 21), 45\} = [0, 31]$, level 1 details: (blk_i, blk_j) , $blk_i, blk_j \in [0, 1]$ $ROI_0 = \{(10, 10), 45\} = [0, 15]$, average blocks: (blk_i, blk_j) , $blk_i, blk_j \in [0, 1]$.

Figure 5 illustrates in 2D using a Wavelet foveated image, each circle represents one data block with size $8 * 8$. Circles in black are data blocks that belongs to ROI_i , $i \in [0, 3]$. Figure 6 and 7 show the procedure of the first and second transmission methods, separately. Black circles represents data blocks being sent in each step. In method 2, there are only 2 steps rather than 4. That is because we use a blockwise structure, each block is regarded as an atomic unit. During each iteration, we may send more data than there is actually needed to reconstruct ROI_i . Thus, detail coordinates needed in step 3 and 4 have been sent in previous steps as redundant data.

3.3 Progressive volume rendering

3.3.1 Rendering with orthogonal viewing direction

Corresponding to the two progressive transmission methods, there are two ways of rendering: region-based and coarse-to-fine.

Algorithm 1: region-based

- *Partial Volume reconstruction*
Given a starting and ending coordinate $(begin_x, begin_y, begin_z)$ and (end_x, end_y, end_z) of a volume and a desired resolution scale 2^k (as a power of 2). We

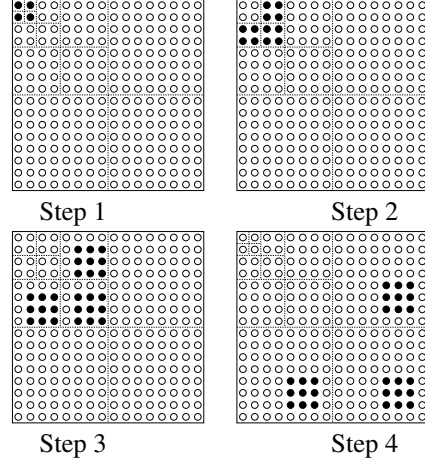


Figure 6: Four iterations of the region-based method.

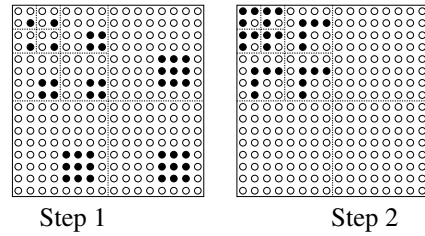


Figure 7: Two iterations of the coarse-to-fine method.

determine its Wavelet coefficients in each layer and reconstruct the original volume data at a desired resolution.

Define the average image and inner most layer to be layer 0 and outer most layer, that is, the desired resolution layer, to be layer l . Wavelet coefficients at layer i is from $(begin_x/2^{(l-i)}, begin_y/2^{(l-i)}, begin_z/2^{(l-i)})$ to $(end_x/2^{(l-i)}, end_y/2^{(l-i)}, end_z/2^{(l-i)})$. Reconstruction starts from the average image and the inner most detail coefficients until desired resolution is reached.

- *Progressive rendering*

Given a mask with `Mask_size=(s,s,s)`, `Mask_center=(x,y,z)`, `num_layer=L` and `min_length=minlen`. In the first iteration, the center fovea is reconstructed and rendered using partial volume reconstruction, which is described in previous section. In a later iteration i , 6 sub-volumes: top, bottom, left, right, front and back are separately reconstructed at a resolution scale 2^{i-1} , rendered using standard rendering algorithm and combine the rendered result to previous rendering image.

- *Image composition*

The top, bottom, left and right rendering images obtained in each iteration are simply added to the previous render-

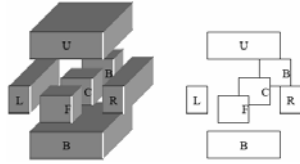


Figure 8: Image composition.

ing image at their right position, while front and back image needs image composition (Figure 8). For each rendering result, the system obtains both density value and alpha value of each pixel. An *over* operator is performed on front, inner and back image, that is, (*front*) *over* (*inner*) *over* (*back*).

over operator can be performed pixel by pixel. Given image pixel $A(d_a, \alpha_a)$ and $B(d_b, \alpha_b)$. Resulting pixel is $C(d_c, \alpha_c)$, where $C = (A)over(B)$ and $d_c = d_a + (1 - \alpha_a) * d_b$.

Algorithm 2: coarse-to-fine

Definition of ROI_0 to $ROI_{m,l}$ are exactly as described in algorithm 1. We start the rendering procedure from ROI_0 , which is the average block to the inner most layer $ROI_{m,l}$. Each layer, exclude the inner most layer $ROI_{m,l}$, can be divided into seven parts, denoted as, *Top*, *Bottom*, *Left*, *Right*, *Front*, *Back* and *Center*. The *Center* part is actually the average information for the inner layer and will be kept for the next iteration. The process is as follows:

Take layer i ROI_i as an example, which is constructed by the *Center* part of ROI_{i-1} and level i detail coefficients. It is divided into seven parts and rendered. In ROI_i , the number of voxels each voxel represent is $2^{m,l-i}$, so the intensity for each voxel in ROI_i is $I = \sum_{i=1}^{2^{m,l-i}} q\alpha(1 - \alpha)^{i-1}$.

Seven parts will be rendered separately and integrated. The center part C_i and the rendering results of *Front* and *Back* RF_i and RB_i parts will be taken down for the next iteration. C_i is the average pass for iteration $i + 1$, and the rendering result of iteration $i + 1$, R_{i+1} , will be combined with RF_i and RB_i using the following equation to refine the rendering result of iteration i . $R = (RF_i + (1 - \alpha)RF_i) * R_{i+1} + (1 - \alpha)RF_i * \alpha R_{i+1} * RB_i$ Repeat this procedure until the inner most layer is reached.

3.3.2 Rendering when viewing from a non-orthogonal viewing direction

When viewing from a non-orthogonal direction, the volume transformation can be simplified by transform each slice to an intermediate coordinate system, sheared object space, for which there is a very simple mapping from the object coordinate system and allows efficient projection. Then warp the intermediate image to the image plane to produce the final result.

Given a viewing direction θ , adjacent voxel slice distance b and adjacent pixel distance d , the rotation can be approximated by shifting each slice to the right by a distance of

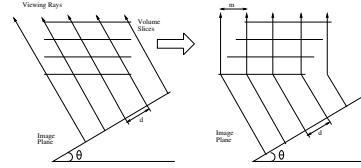


Figure 9: Volume being transformed to sheared object space.



Figure 10: Direct rendering result.

$l = b * \tan \theta$. To ensure the pixel distance in the resulting image is still d after shearing, the ray distance in the sheared object coordinate should be $m = d / \cos \theta$ (Figure 9). After shearing, re-sampling by interpolation should be performed to get the voxel density value along the viewing ray.

In our schemes, we use Wavelet shear-warp factorization. The difference with the above shear-warp algorithm is we perform it in the Wavelet domain instead of spatial domain. Factorization of the low sub-band LLL_i coefficients in fovea area in each level will approximate that of the whole volume. As mentioned above, coefficients in fovea area of all levels is approximately 2000 times smaller than the original volume data size, thus Wavelet shear-warp avoids tedious shearing of the whole data set and tremendously reduces the computational complexity. After shearing of Wavelet coefficients, they will be input to the algorithm mentioned in orthogonal rendering and produce an intermediate image by normal projection. Warp function will then be executed on the intermediate image to produce the final image.

4 Experimental study

In our experiment, we use cross-section of human head as our example. The size of the volume data is 256^3 , size of the average image is 16^3 , thus $m,l = \log_2(256/16) = 4$. Wavelet volume W is divided into blocks of size 8^3 . Given $mask_center = \{128, 128, 128\}$ and $mask_size = \{50, 50, 50\}$, we will compare in each iteration, the result image, data amount being transmitted and time of two schemes.

The experiment showed that, in the first region-based algorithm. The client can see his most interested region-of-interest(ROI) at the first iteration. and the client will have to

Experiment Results				
		Data(int)	Image	Trans/Render(s)
Itr	Sche1	529,054	Fig 11(a)	0.381/0.0472
	Sche2	56,564	Fig 12(a)	0.1468/0.047
Itr	Sche1	384,860	Fig 11(b)	0.125/0.0154
	Sche2	353,946	Fig 12(b)	0.1154/0.0222
Itr	Sche1	296,938	Fig 11(c)	0.0938/0.0156
	Sche2	440,340	Fig 12(c)	0.1404/0.0156
Itr	Sche1	0	Fig 11(d)	0.0/0.0
	Sche2	360,002	Fig 12(d)	0.1092/0.0158
Sum	Sche1	1,210,852	-	0.5998/0.0782
	Sche2	1,210,852	-	0.5118/0.1006

Table 3: Experiment results of the two progressive rendering schemes.

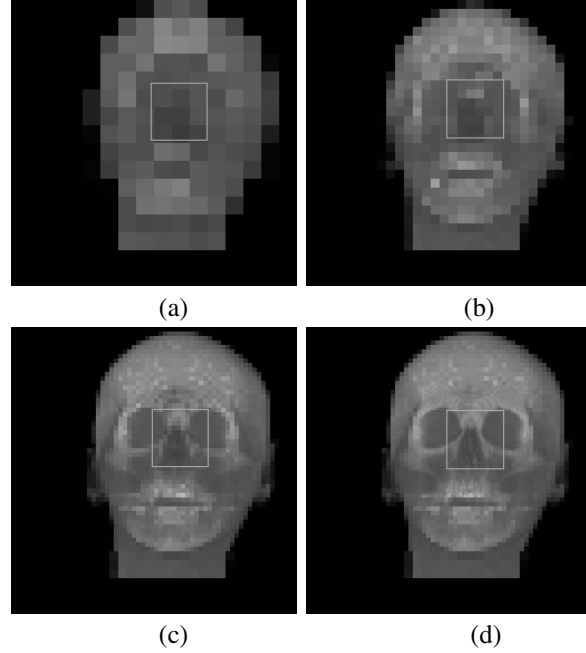


Figure 12: Four iterations of the coarse-to-fine scheme.

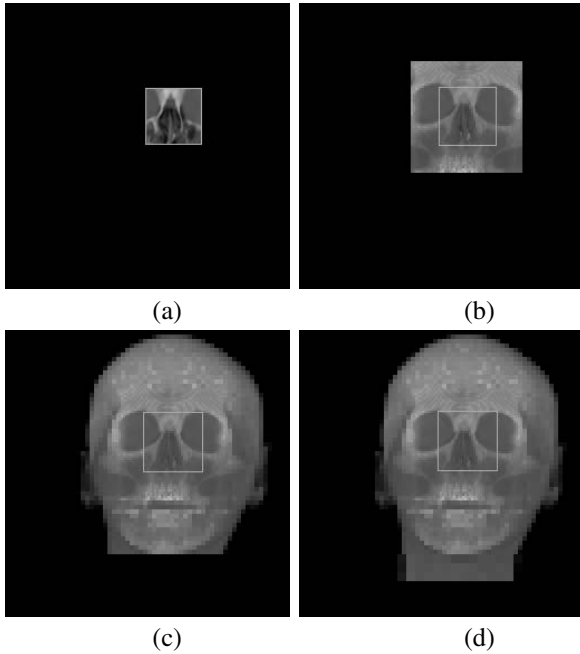


Figure 11: Four iterations of the region-based scheme.

wait more than two times of the time (0.5118 second comparing to 0.381 second) for the inner most ROI to arrive in second algorithm: coarse-to-fine, which is not desirable. Furthermore, region-based rendering algorithm can give a clearer rendering result of ROI. In coarse-to-fine algorithm, low resolution details arrive first and high resolution inner layer arrives later. Thus its clarity will be interfered by low resolution coefficients. However, the client waits less time for the first rendering result to be displayed on the client site in coarse-to-fine algorithm, 0.1468 second comparing to 0.381 second. ROI is highlighted with a square in each figure.

Another example we take here is cross-section of human dummy with size 256^3 . Size of the average image is 16^3 , $m_l = 4$. Given $mask_center = 128, 128, 128$ and $mask_size = 50, 50, 50$. (Figure 13 and Figure 14)

5 Conclusion

Our work in this paper aimed at accessing to large scale volume data stored on server repository and progressively rendered on client site in multiresolution. In our solution, there are two ways of progressive transmission/rendering: region-based and coarse-to-fine schemes. They are based on Wavelet foveation. The experimental study confirmed the effectiveness of the solution.

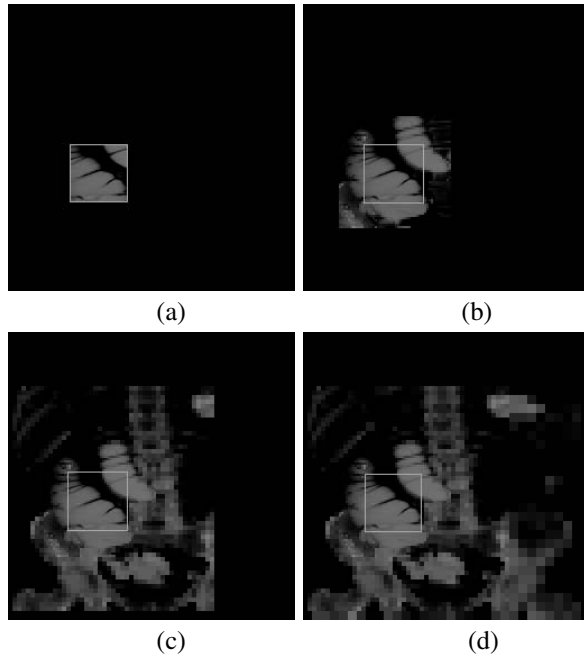


Figure 13: Four iterations of the region-based scheme.

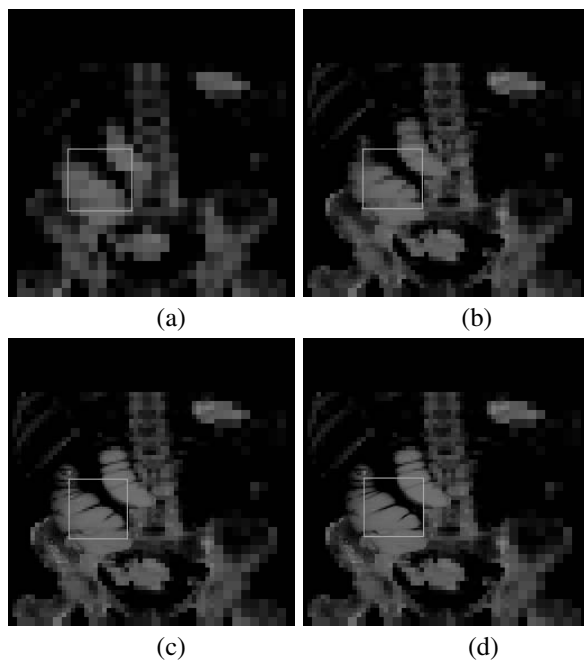


Figure 14: Four iterations of the coarse-to-fine scheme.

REFERENCES

- Bhaniramka, P. and Demange, Y. (2002). Opengl volumizer: a toolkit for high quality volume rendering of large data sets. In *Proc. of IEEE VolVis*, pages 45–54.
- Chang, E. C., Mallat, S., and Yap, C. (2000). Wavelet foveation. *Applied and Computational Harmonic Analysis*, 3(4):312–336.
- Engel, K., Kraus, M., and Ertl, T. (2001). High-quality pre-integrated volume rendering using hardware-accelerated pixel shading. In *Proc. of Eurographics / SIGGRAPH Workshop on Graphics Hardware*, pages 9–16.
- Gross, M. H., Lippert, L., Dittrich, R., and Haring, S. (1997). Two methods for wavelet-based volume rendering. *Computer & Graphics*, 21(2):237–252.
- Guthe, S., Wand, M., Gonser, J., and Strasser, W. (2002). Interactive rendering of large volume data sets. In *Proc. of IEEE Visualization*, pages 53–60.
- Hancock, D. J. and Hubbold, R. J. (1997). Efficient image synthesis on distributed architectures. In R. Earnshaw and J. Vince, editors, *The Internet in 3D, Information, Images and Interaction*, Academic Press, pages 347–364.
- Ihm, I. and Park, S. (1998). Wavelet-based 3d compression scheme for very large volume data. In *Proc. of Graphics Interface*, pages 107–116.
- Kim, T. and Shin, Y. (1999). An efficient wavelet-based compression method for volume rendering. In *Proc. of Pacific Graphics*, pages 147–156.
- Lacroute, P. and Levoy, M. (1994). Fast volume rendering using a shear-warp factorization of the viewing transformation. In *Proc. of SIGGRAPH*, pages 451–458.
- Meissner, M., Huang, J., Bartz, D., Mueller, K., and Crawfis, R. (2000). A practical evaluation of popular volume rendering algorithms. In *Proc. of IEEE VolVis*, pages 81–88.
- Norton, A. and Rockwood, A. P. (March 2003). Enabling view-dependent progressive volume visualization on the grid. *IEEE Computer Graphics and Applications*, 23(2):22–31.
- Pinnamaneni, P. (2003). *Wavelet-Based Volume Rendering*. PhD thesis, Mississippi State University.
- Pinnamaneni, P., Saladi, S., and Meyer, J. (2002). Remote transformation and local 3d reconstruction and visualization of biomedical data sets in java3d. In *Proc. of SPIE Visualization and Data Analysis 2002*, volume 2, pages 44–54.
- Westenberg, M. A. and Roerdink, J. B. (2000). X-ray volume rendering by hierarchical wavelet splatting. In *Proc. of ICPR*, volume 3, page 3163.
- Westover, L. (1990). Footprint evaluation for volume rendering. In *Proc. of the 17th annual conference on Computer graphics and interactive techniques*, pages 367–376.